

# Direct Low-Potential Electropolymerization of 9,10-Dihydrophenanthrene in Boron Trifluoride Diethyl Etherate

Guangming Nie, Liangjie Zhou, Yan Zhang, Jingkun Xu

Key Laboratory of Eco-Chemical Engineering, Ministry of Education; College of Chemistry and Molecular Engineering, Qingdao University of Science and Technology, Qingdao 266042, People's Republic of China

Received 17 January 2009; accepted 1 July 2009

DOI 10.1002/app.31078

Published online 26 March 2010 in Wiley InterScience (www.interscience.wiley.com).

**ABSTRACT:** High-quality poly(9,10-dihydrophenanthrene) (PPh) with good fluorescence properties was synthesized electrochemically by the direct anodic oxidation of 9,10-dihydrophenanthrene in boron trifluoride diethyl etherate (BFEE). PPh films obtained from BFEE-based electrolytes showed good electrochemical behavior and good thermal stability with an electrical conductivity of  $2.2 \times 10^{-3}$  S/cm; this indicated that BFEE was a better medium for the electrosyntheses of PPh films. Dedoped PPh films were soluble in  $\text{CH}_2\text{Cl}_2$ , dimethylformamide, and dimethyl

sulfoxide. The structure and morphology of the polymer were also characterized by ultraviolet–visible spectroscopy, Fourier transform infrared spectroscopy,  $^1\text{H-NMR}$  spectroscopy, and scanning electron microscopy, respectively, which indicated the polymerization mainly occurred at the  $\text{C}_{(2)}$  and  $\text{C}_{(7)}$  positions. Fluorescent spectral studies indicated that PPh was a good blue-light emitter. © 2010 Wiley Periodicals, Inc. *J Appl Polym Sci* 117: 793–800, 2010

**Key words:** conducting polymers; electrochemistry

## INTRODUCTION

Extensive work has been carried out on studying conducting  $\pi$ -conjugated polymers because of their wide fundamental interest and potential industrial applications. Recently, polycyclic aromatic hydrocarbons such as poly(*para*-phenylene),<sup>1</sup> polyfluorene,<sup>2,3</sup> and polyphenanthrene<sup>4,5</sup> have been investigated. Poly(*para*-phenylene) obtained from benzene<sup>6</sup> or with dissolved biphenyl<sup>7</sup> as the starting material under mild conditions is one of the simplest conjugated polymers with a high stability and moderate electrical conductivity. Polyfluorene, with a methylene-type bridge in poly(*para*-phenylene), has been widely investigated for applications in the emissive layers in light-emitting diodes (LEDs) because of its high chemical and thermal stability and high fluorescence quantum yields.<sup>3</sup> Polyphenanthrene, representing the simplest tricyclic aromatic hydrocarbons,

has been studied theoretically because of its great technological importance as an electrode material for lithium-ion rechargeable batteries.<sup>4,5</sup>

However, to date, there have only been a few publications<sup>8,9</sup> concerned with polymers prepared from 9,10-dihydrophenanthrene (Ph; Scheme 1) with an ethylene-type bridge in the poly(*para*-phenylene). At the very start, Saito et al.<sup>8</sup> reported the preparation of poly(9,10-dihydrophenanthrene) (PPh) obtained from 2,7-dibromo-9,10-dihydrophenanthrene with an isolated zero-valent nickel complex and an electrochemically generated zero-valent nickel complex. This polymer was insoluble and did not melt, which prevented detailed analysis of the properties of the polymer. Subsequently, to enhance the solubility of the polymer, Yamamoto et al.<sup>9</sup> obtained soluble PPh from Ph derivatives, introducing substituents at the 9 and 10 positions, such as  $-\text{OSi}(\text{R})_2(\text{R}')$  groups, by the dehalogenative polycondensation of the corresponding monomers via the use of a zero-valent nickel complex. Until now, PPh has mainly been prepared from Ph derivatives via a precursor route by means of a chemical method. The pursuit of high-quality polymer films is still one of the main goals in the research and development of inherently conducting polymers. Electrochemical polymerization has been proven to be one of the most useful approaches for conducting polymer synthesis with several advantages, such as one-step deposition on the working electrode, the amount of polymer being controlled by the integrated charge passed through

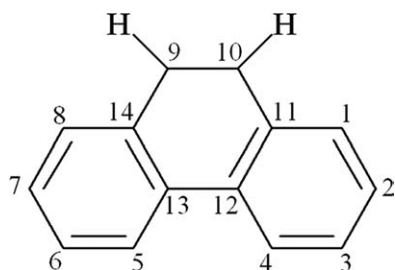
Correspondence to: G. Nie (gmnie@126.com).

Contract grant sponsor: Natural Science Foundation of Shandong Province; contract grant number: Y2007B22.

Contract grant sponsor: Scientific and Technical Development Project of Qingdao; contract grant number: 07-2-3-11-jch.

Contract grant sponsor: National Natural Science Foundation of China; contract grant numbers: 20775038, 50663001.

*Journal of Applied Polymer Science*, Vol. 117, 793–800 (2010)  
© 2010 Wiley Periodicals, Inc.



Scheme 1 Structural formula of Ph.

the cell, and only small amounts of monomer required. In addition, electrochemical studies can give fast information on the characteristics and properties of electropolymerized materials with good accuracy and precision. With this in mind, it was interesting to prepare high-quality PPh films by the direct electrochemical polymerization of the Ph monomer. There were no other reports on the electrochemical polymerization of the Ph monomer directly in boron trifluoride diethyl etherate (BFEE) except for one article.<sup>10</sup>

It is well known that free-standing films of polythiophene and its derivatives,<sup>11,12</sup> poly(*para*-phenylene),<sup>13</sup> and polyfluorene and its derivatives<sup>14–16</sup> can be produced by the direct anodic oxidation of the corresponding monomers in BFEE with better properties. Under these circumstances, BFEE serves not only as the solvent and but also as the supporting electrolyte, and no other supporting electrolyte is needed.<sup>17</sup> On the other hand, BFEE can exist in diethyl ether as a polar molecule,  $[(C_2H_5)_3O]^+BF_4^-$ , which furnishes a conducting medium. This solution is also electrochemically stable over a wide potential range.

In this study, high-quality PPh films were easily prepared by the anodic oxidation of the Ph monomer directly in BFEE. The electrochemical properties, conductivity, polymerization mechanism, optical properties, morphology, and thermal properties of the as-prepared PPh were investigated.

## EXPERIMENTAL

### Materials

Ph (Acros Organics, 99%, Geel, Belgium) was used as received. BFEE (Beijing Changyang Chemical Plant, Beijing, China) was distilled and stored at  $-20^\circ\text{C}$  before use. Tetrabutylammonium tetrafluoroborate (TBATFB; Acros Organics, 95%, Geel, Belgium) was dried *in vacuo* at  $60^\circ\text{C}$  for 24 h before use. Commercial high performance liquid chromatography (HPLC)-grade acetonitrile (ACN; made by Shandong Laiyang Chemical Research Institute, Laiyang, China) was dried by a molecular sieve before use. Sulfuric acid (98%) and 25% ammonia, made by

Jinan Chemical Reagent Co. (Jinan, China), were used as received. Dimethyl sulfoxide (DMSO; analytical reagent, Tianjin RuiJinte Chemical Plant, Tianjin, China) was also used as received. Deuterium-substituted dimethyl sulfoxide ( $CD_3SOCD_3$ ) was a product of Cambridge Isotope Laboratory, Inc. (Andover, MA).

### Electrosyntheses of the PPh films

Electrochemical syntheses and examinations were performed in a one-compartment cell with the use of a model 263 potentiostat–galvanostat (EG&G Princeton Applied Research, Oak Ridge, TN) under computer control. The working and counter electrodes for cyclic voltammetry (CV) experiments were platinum wires with a diameter of 0.5 mm placed 0.5 cm apart. To obtain a sufficient amount of polymer for characterizations, stainless steel sheets with surface areas of 10 and 12  $\text{cm}^2$  each were used as the working and counter electrodes, respectively. The electrodes mentioned previously were carefully polished with abrasive paper (1500 mesh) and cleaned by water and acetone successively before each examination. All of the potentials were referred to a saturated calomel electrode (SCE).

The typical electrolytic solution was BFEE containing 0.1 mol/L Ph monomer. All of the solutions were deaerated by a dry argon stream and maintained at a slight argon overpressure during the experiments. The amount of polymer deposited on the electrode was controlled by the integrated charge passed through the cell. To remove the electrolyte and oligomers/monomer, as-formed polymer films were rinsed in mixtures of acetone and water. For spectral analysis, the polymer was dedoped with 25% ammonia for 3 days at room temperature and then washed repeatedly with acetone. Finally, it was dried *in vacuo* at  $60^\circ\text{C}$  for 2 days.

### Characterizations

We measured the current efficiency ( $\eta$ ) of polymerization (the charge consumed by the growth of polymer film relative to the total charge passed through the cell) by weighing the polymer (in a dedoped state) deposited on the electrode ( $W_p$ ) according to eq. (1):

$$\eta = [(nFW_p/M)/Q] \times 100\% \quad (1)$$

where  $F$  is the Faraday constant (96,487 C/mol),  $Q$  is the integrated charge passed through the cell during film growth,  $n$  is the number of electrons transferred per monomer attached to the polymer (where  $n$  was estimated to be 2), and  $M$  is the molar mass of the monomer. To calculate  $\eta$  of the anodic polymeriza-

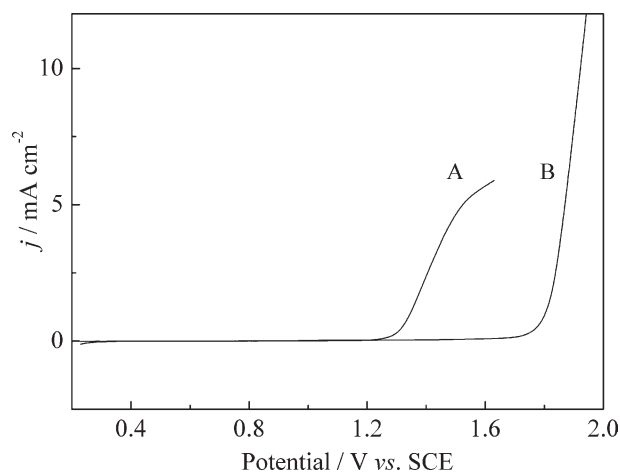


**Figure 1** Anodic polarization curves of (A) 0.1 mol/L Ph in BFEE and (B) ACN+0.1 mol/L TBATFB (potential scan rate = 20 mV/s).

tion, the total  $Q$  during the polymerization was used. In this experiment, this value contained charges used in both the electrochemical polymerization and doping process.  $\eta$  of this electrosynthesis was determined to be 66%. The doping level ( $f$ ) of the as-grown PPh films was 16%, which was determined electrochemically with eq. (2).<sup>18</sup>

$$f = [2Q_o / (\eta Q_d - Q_o)] \times 100\% \quad (2)$$

where  $Q_d$  is the total charge used for PPh deposition and  $Q_o$  is the total charge of oxidized species in the PPh films.

The conductivity of the as-formed PPh film was measured by the conventional four-probe technique. Ultraviolet-visible (UV-vis) spectra were taken with a Cary 50 UV-vis-near infrared spectrophotometer (Mulgrave Victoria, Australia). IR spectra were recorded with a Nicolet 510P Fourier transform infrared (FTIR) spectrometer (Bremen, Germany) with KBr pellets. The <sup>1</sup>H-NMR spectrum was recorded on a JEOL GAM-ECP600 NMR spectrometer (Fällanden, Switzerland), and CD<sub>3</sub>SOCD<sub>3</sub> was used as the solvent. The thermogravimetric analysis (TGA) was performed with a NETZSCH TG209 thermal analyzer (Selb, Germany). All thermal analyses were performed under a nitrogen stream in the temperature range 295–1173 K with a heating rate of 10 K/min. Scanning electron microscopy (SEM) measurements were taken with a JEOL JSM-6700F scanning electron microscope (Tokyo, Japan). The fluorescence spectra were determined with an F-4500 fluorescence spectrophotometer (Hitachi, Japan). The fluorescence quantum yields ( $\Phi$ 's) of PPh in solution was measured with anthracene in ACN (standard,  $\Phi_{\text{ref}} = 0.27$ )<sup>19</sup> as a reference and was calcu-

lated according to the well-known method given in eq. (3):

$$\Phi_{\text{overall}} = (n^2 A_{\text{ref}} I / n_{\text{ref}}^2 A I_{\text{ref}}) \times \Phi_{\text{ref}} \quad (3)$$

where  $n$ ,  $A$ , and  $I$  denote the refractive index of the solvent, the absorbance at the excitation (EX) wavelength, and the intensity of the emission (EM) spectrum, respectively. The subscript *ref* denotes the reference, and no subscript denotes the sample. The absorbance of the samples and the standard should be similar.<sup>20</sup>

## RESULTS AND DISCUSSION

### Electrochemical polymerizations

Figure 1 shows the anodic polarization curves of Ph in BFEE [Fig. 1(A)] and in ACN containing 0.1 mol/L TBATFB [Fig. 1(B)], respectively. The polymerization of Ph was first investigated in ACN containing 0.1 mol/L TBATFB, in which the oxidation onset of Ph was initiated at 1.75 V versus SCE. However, the onset of oxidation was 1.35 V versus SCE in pure BFEE, which was much lower than that of Ph in ACN/TBATFB. This implied that the oxidation of Ph in BFEE was easier than that in ACN/TBATFB. The interactions between BFEE and Ph lowered their oxidation potentials, and the catalytic effect of BFEE also facilitated the oxidation of monomer. BFEE was electrochemically silent in the whole potential range. Generally, the lower the oxidation potential is, the less possible are the side polymerization reactions as well as coupling defects. Therefore, BFEE was more appropriate for the electrochemical polymerization of Ph.

The successive CV scans of 0.1 mol/L Ph in BFEE are shown in Figure 2(A). As shown in this figure,

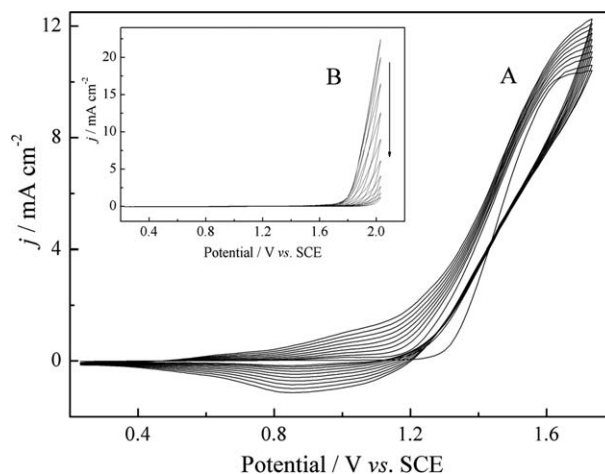


**Figure 2** CV scans of 0.1 mol/L Ph in BFEE and ACN+0.1 mol/L TBATFB (inset; potential scan rates = 100 mV/s).

CV of Ph in BFEE showed the characteristic features as other conducting polymers during potentiodynamic syntheses. As the CV scan continued, a polymer film was also formed on the working electrode surface. The increase in the redox wave currents implied that the amount of the polymer on the electrode was increasing. The broad redox waves of the as-formed PPh film was ascribable to the wide distribution of the polymer chain length<sup>21</sup> or the conversion of conductive species on the polymer main chain from the neutral state to polarons, from polarons to bipolarons, and finally from bipolarons to the metallic state.<sup>22</sup> All of these phenomena indicated that a high-quality conducting PPh film was formed on the working electrode. On the other hand, the successive CV scans of Ph in ACN containing 0.1 mol/L TBATFB was not very successful, and there was no polymer film formed on the electrode [Fig. 2(B)], which indicated it was hard to obtain PPh films by the anodic oxidation of Ph directly in the ACN/TBATFB system. The anodic current wave decreased quickly with increasing CV scan number, and no apparent redox waves were found. In other words, this method was not suitable for PPh deposition. From this point of view, BFEE was a better medium for the electrosyntheses of conducting PPh films.

### Electrochemistry of the PPh films

To get a deeper insight into the electrochemical and environmental stabilities of the PPh films and their electroactive behaviors, the electrochemical behaviors of the PPh films deposited electrochemically from BFEE were studied both in monomer-free BFEE [Fig. 3(A)] and in concentrated sulfuric acid [Fig. 3(B)]. The steady-state CV scans represented broad anodic and cathodic peaks. The peak current densities were both proportional to the scan rates (Fig. 3, inset), which indicated that the process was not diffusion-controlled and that film was present on the electrode surface. According to Figure 3(A), the PPh film could be oxidized and reduced in monomer-free BFEE from 1.2 ( $E_{a'}$ , anodic peak potential) to 0.8 V ( $E_{c'}$ , cathodic peak potential). In addition, the CV scans showed a pronounced hysteresis,<sup>23,24</sup> that is, a considerable difference between the anodic and cathodic peak potentials, respectively. However, the anodic and cathodic peak potentials of these films in concentrated sulfuric acid were independent of the scan rates [Fig. 3(B)]. In addition, much lower potentials, from 0.75 ( $E_a$ ) to 0.55 V ( $E_c$ ), were needed to oxidize or reduce the polymer film in concentrated sulfuric acid [Fig. 3(B)]. The difference of ( $E_a - E_c$ ), related to the kinetics of the doping–dedoping reaction,<sup>25</sup> was equal to 0.2 V for PPh in concentrated sulfuric acid and up to 0.4 V for PPh in monomer-free BFEE. From these results, we could

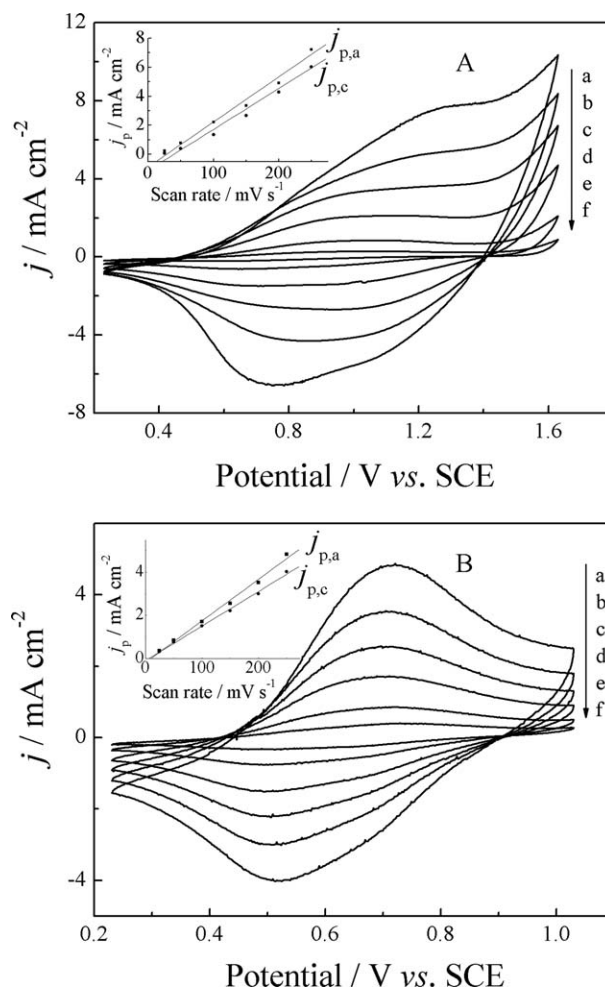


**Figure 3** CV scans of the PPh film in the (A) monomer-free BFEE and (B) concentrated sulfuric acid at potential scan rates of (a) 250, (b) 200, (c) 150, (d) 100, (e) 50, and (f) 25 mV/s. The PPh film was synthesized electrochemically in pure BFEE at a constant applied potential of 1.3 V versus SCE.  $j_{p,a}$ , anodic peak current density;  $j_{p,c}$ , cathodic peak current density;  $j_p$ , peak current density; V, volt; j, current density.

reasonably conclude that the doping–dedoping reaction of PPh in concentrated sulfuric acid was faster than in monomer-free BFEE, which may have been attributed to the different doping anions during the process of successive CV scans. The doping anions ( $\text{HSO}_4^-$  or  $\text{SO}_4^{2-}$ ) in concentrated sulfuric acid moved into and out of the polymer film more easily than  $[(\text{C}_2\text{H}_5)_3\text{O}]^+\text{BF}_4^-$  (the conducting medium in BFEE) in monomer-free BFEE. Therefore, the exchange of the doping anions in and out of the PPh films was faster in  $\text{H}_2\text{SO}_4$  than in monomer-free BFEE. It is well known that the high electrochemical stability of the conducting polymer is important to application in some fields, such as polymeric and organic LEDs.<sup>26</sup> The long-term stability of the redox activity of the PPh film was also investigated in concentrated sulfuric acid. There was no significant decomposition in

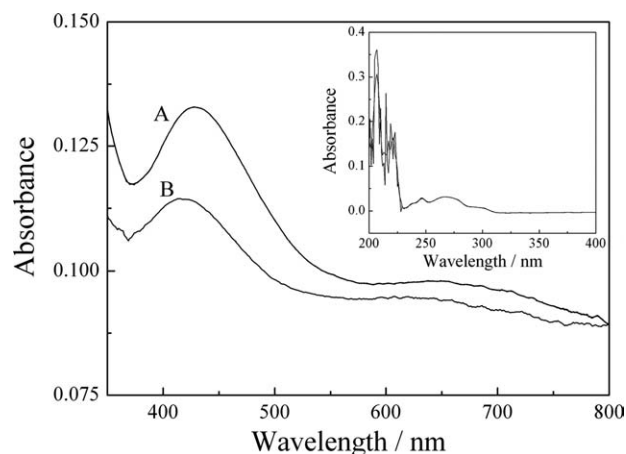


**Figure 4** UV-vis spectra of the Ph monomer (inset) and dedoped PPh films coated on an optically transparent indium tin oxide electrode prepared from BFEE with different deposition charge densities: (A) 0.02 and (B) 0.01 C/cm<sup>2</sup>.

the peak current, which indicated that the PPh film showed better long-term environmental and redox stability. The electrochemical stability will facilitate the application of PPh films prepared from BFEE-based electrolytes.

### Structural characterizations

During the potentiostatic process, the color of BFEE-containing Ph darkened with the applying potential, which indicated that soluble PPh oligomers formed during anodic oxidation. Therefore,  $\eta$  of Ph polymerization was determined to be only 66%. The PPh film was brown in the doped state and was yellow in the dedoped state. The as-formed PPh film was soluble in CH<sub>2</sub>Cl<sub>2</sub>, dimethylformamide, and DMSO. The UV-vis spectra of Ph and PPh on an optically transparent indium tin oxide electrode with different deposition charge densities were examined, as shown in Figure 4. The monomer showed several characteristic absorptions between 200 and 230 nm with a shoulder at 280 nm (Fig. 4, inset). The spectrum of the dedoped PPh films showed a much broader absorption, which indicated a wider molar mass distribution of the as-prepared PPh films during the electrosynthesis. Moreover, a higher deposition charge density favored polymer formation with higher conjugation lengths, as indicated by a redshift of the main absorption from 415 to 435 nm (Fig. 4). Generally, the longer wavelength is the absorption, and the higher conjugation length is the polymer. This result implies that the PPh film prepared from BFEE had conjugated polymer formation with a broad molar mass distribution.

Vibrational spectra can provide structural information on neutral and doped conducting polymers. IR

spectra provided evidence for the existence of the conjugated structure of the PPh chain. Figure 5 displays the transmittance FTIR spectra of the Ph monomer and dedoped PPh obtained from BFEE. The details of the band assignments values supported that dedoped PPh had a  $\pi$ -conjugated system similar to that of poly(*para*-phenylene).<sup>7</sup> The bands at 815 and 882 cm<sup>-1</sup> were assigned to the C-H out-of-plane vibration of the phenyl, and the band at about 1035 cm<sup>-1</sup> was due to the C-H in-plane vibration of the phenyl. These bands were similar to those of 1,2,4-trisubstituted benzene rings with respect to the wave number and the pattern of the absorption bands. Bands at 1625 and 1433 cm<sup>-1</sup> were attributed to C=C aromatic ring vibrations. On the basis of this consideration, we concluded reasonably that the polymerization position of Ph mainly occurred at the C<sub>(2)</sub> and C<sub>(7)</sub> positions (Scheme 2).

To further investigate the polymer structure and the polymerization mechanism of Ph, the <sup>1</sup>H-NMR spectrum of Ph and the dedoped PPh prepared from BFEE were recorded, as shown in Figure 6. The proton lines of PPh [Fig. 6(B)] were much broader than the corresponding proton lines of the monomer [Fig. 6(A)] because of the effect of the formation of a new bond between the Ph monomers and the wide molar mass distribution of PPh. Some new peaks appeared after polymerization, and most of the peaks moved to a lower field, which was mainly because of the introduction of a higher conjugation length in the PPh main chain. As shown in Figure 6(B), the proton chemical shift from about 8.85 to 9.17 was ascribed to the protons at C<sub>(4)</sub> and C<sub>(5)</sub>, and the proton chemical shift from about 7.80 to 8.00 was ascribed to the protons at C<sub>(1)</sub>, C<sub>(3)</sub>, C<sub>(6)</sub>, and C<sub>(8)</sub> (Scheme 1). The origin of the peak at about 7.20 was attributed to the terminal proton in the polymer because of its

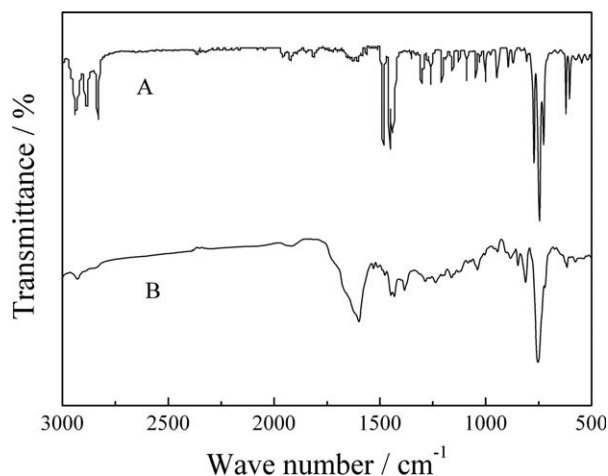
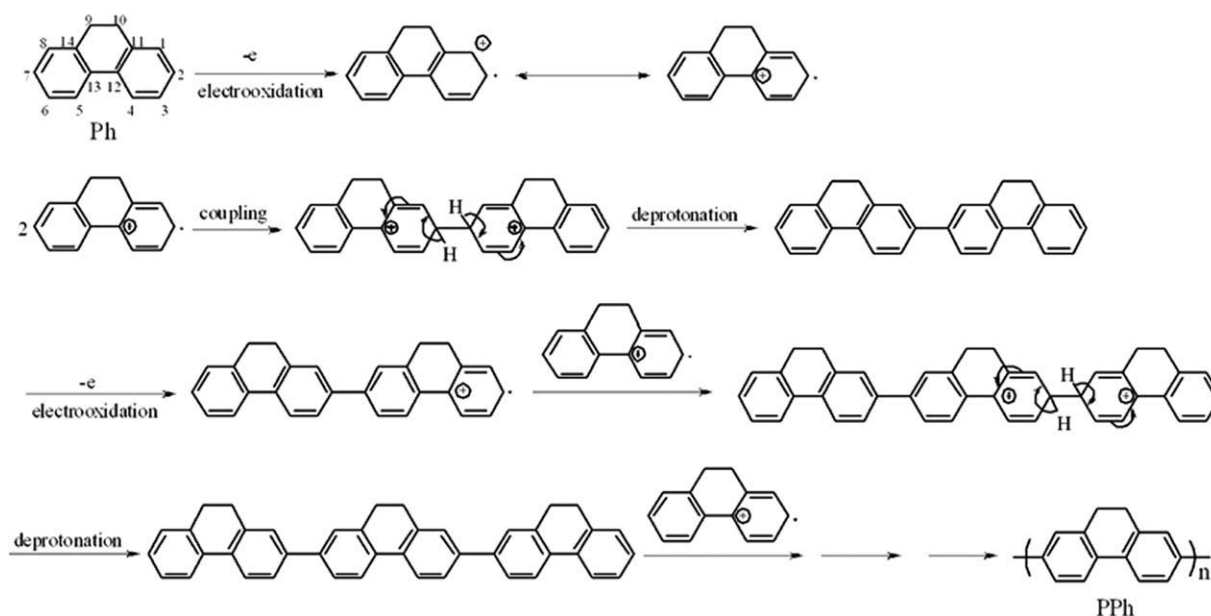


**Figure 5** FTIR spectra of the (A) Ph monomer and (B) PPh obtained potentiostatically at 1.3 V versus SCE from BFEE.



Scheme 2 Possible polymerization mechanism of Ph.

small shift in field relative to those of the peaks of monomer [ $C_{(2)}$  and  $C_{(7)}$ ]. The information, as mentioned previously, indicated that a new C—C bond between two monomers via  $C_{(2)}$  and  $C_{(7)}$  was formed. Under this circumstance, the conjugation through  $C_{(1)}$ ,  $C_{(3)}$ ,  $C_{(6)}$ ,  $C_{(8)}$ ,  $C_{(4)}$ , and  $C_{(5)}$  were enhanced after polymerization, which made the chemical shift of the protons on these atoms move to a lower field. The proton chemical shift at 2.80 was ascribed to the protons of  $C_{(9)}$  and  $C_{(10)}$  (Fig. 6). On the basis of the  $^1\text{H-NMR}$  spectra, we reasonably concluded that the polymerization of the Ph ring mainly occurred at the  $C_{(2)}$  and  $C_{(7)}$  positions, which was in accordance with the results of polymer structure mentioned previously. The proposed polymerization mechanism of Ph is illustrated in Scheme 2. As shown in Scheme 2, according to the mechanism of radical–radical coupling, upon its oxidation, a neutral Ph monomer yields cation radical species, which then recombine to yield consecutively a dihydrodimerdication as an intermediate product. Then, a new dimer is obtained after its disproportionation process. The dimer undergoes further oxidation, recombination, and deprotonation steps, which lead to the oxidative polymer end product (PPh).

The fluorescence properties of the dedoped PPh were examined with DMSO as the solvent, as shown in Figure 7. The three-dimensional scans of EX–EM–intensity are shown in Figure 7(A). EM and EX spectra of dedoped PPh [Fig. 7(B)] and monomer [Fig. 7(B), inset] were also recorded. According to Figure 7(B), the monomer showed an EX spectra at 280 nm [Fig. 7(B), inset], and the EX spectra of PPh was mainly found at 370, 417, and 445 nm. On the other hand, there was one peak of the EM spectrum of the mono-

mer at 340 nm [Fig. 7(B), inset], whereas the obvious peaks of the EM spectra of PPh were mainly located at 450 and 500 nm. The wide EX and EM spectra were ascribed to the wide molar mass distribution of PPh, in accordance with the UV–vis spectra. The fluorescence quantum yield of as-formed PPh in DMSO was measured to be 0.76 according to eq. (3). This value was higher than that of poly(9,10-dihydrophenanthrene-2,7-diyl)s with  $-\text{OSiMe}_2\text{Ocd}$  synthesized by dehalogenative polycondensation with a zero-valent nickel complex ( $=0.62$ ).<sup>9</sup> The results indicate that the polymer was a good blue-light emitter and also show that PPh may have some potential application in various fields, such as organic lasers with blue-emitting polymers and blue–violet polymer LEDs.

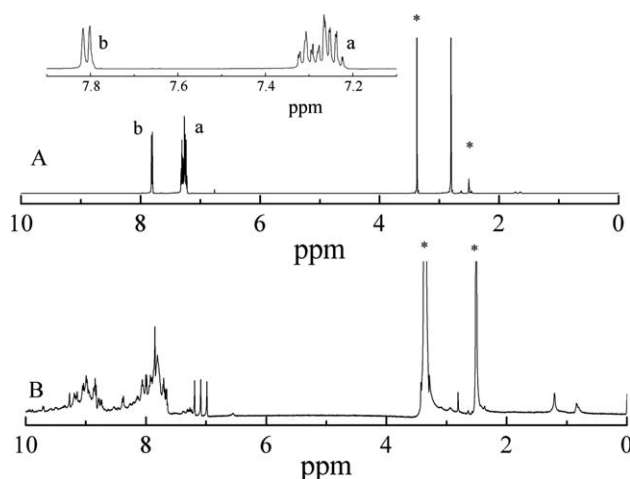


**Figure 6**  $^1\text{H-NMR}$  spectra of the (A) Ph monomer and (B) dedoped PPh prepared potentiostatically at 1.3 V versus SCE from BFEE (solvent:  $\text{CD}_3\text{SOCD}_3$ ). Peaks with an asterisk represent the spectra of the solvent.

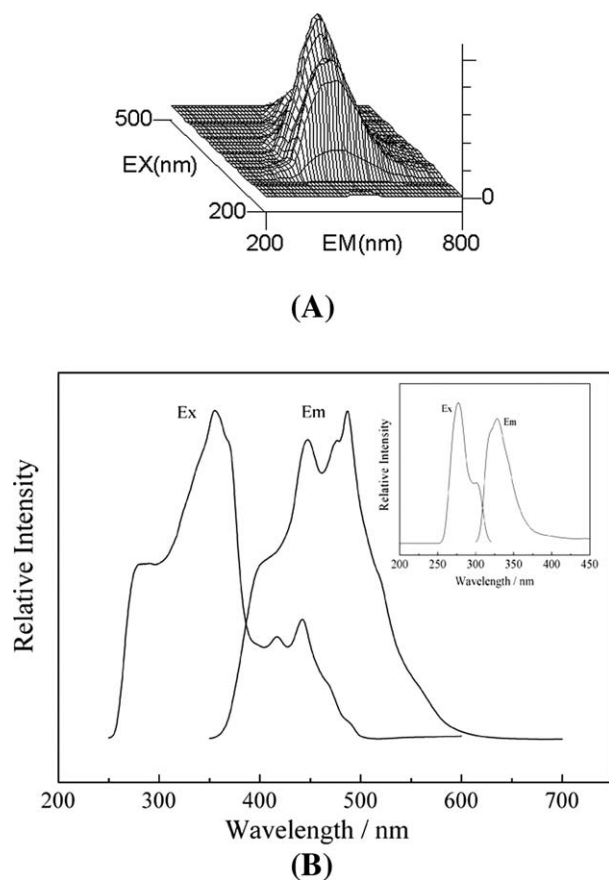


**Figure 7** (A) Three-dimensional scans of EX–EM–intensity of the dedoped PPh and EM and EX spectra of the (B) dedoped PPh and (B, inset) Ph monomer (solvent: DMSO).

### Thermal analysis

The thermal stability of a conducting polymer is very important for its potential application. TGA is a significant and useful dynamic way to detect the degradation behavior in which the weight loss of a

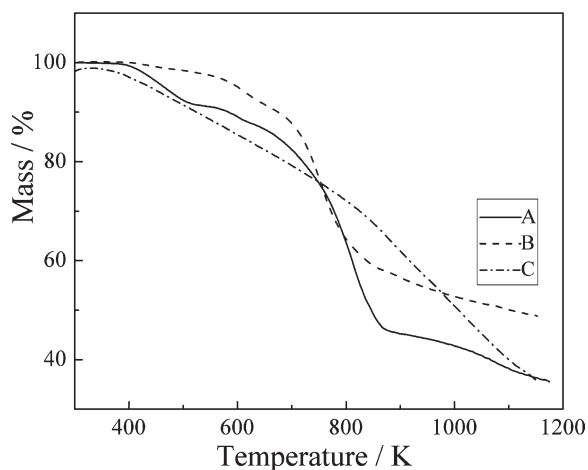


**Figure 8** TGA curves of the (B) dedoped PPh obtained potentiostatically at 1.3 V versus SCE from BFEE and dedoped poly(*para*-phenylene) obtained from (A) biphenyl and (C) benzene.

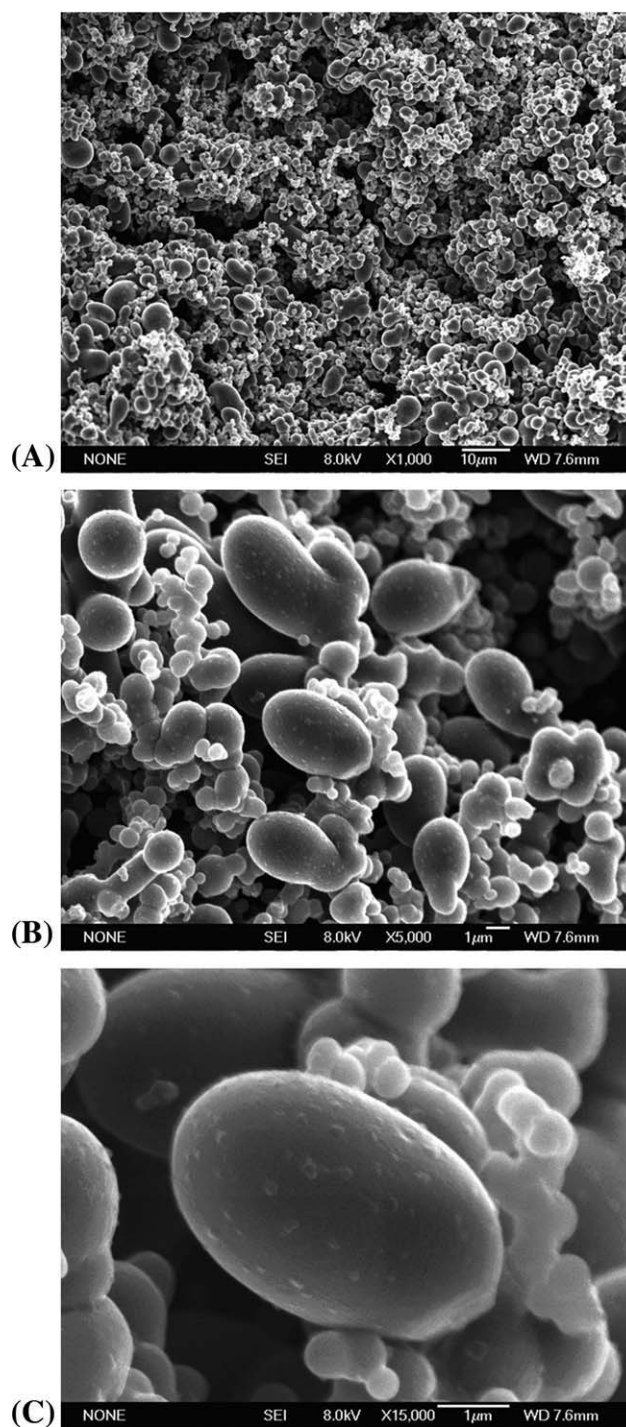


**Figure 9** SEM micrographs of the PPh film with different objective amplifications with magnifications of (A) 1000, (B) 5000, and (C) 15,000 diameters deposited electrochemically on the electrode surface obtained from BFEE potentiostatically at 1.3 V versus SCE.

polymer sample is measured continuously while the temperature is changed at a constant rate. To investigate the thermal stability of the PPh films prepared from BFEE, the thermal analysis of the PPh films was performed, as shown in Figure 8(B). For comparison, the thermal properties of poly(*para*-

phenylene) obtained from benzene [Fig. 8(C)] and biphenyl [Fig. 8(A)] were also investigated under the same conditions. According to Figure 8(B), it is clear that PPh started to lose weight obviously when the temperature reached 720 K. However, there were two evident decomposition processes during the thermal degradation of poly(*para*-phenylene) obtained from biphenyl [Fig. 8(A)], these two decompositions occurred at 400 and 660 K. This indicated that PPh had a better thermal stability than poly(*para*-phenylene) obtained from biphenyl. According to Figure 8(C), the poly(*para*-phenylene) film obtained from benzene had a lower decomposition temperature, and there was no prominent maximum decomposition rate in the whole process. In addition, the residual weight of PPh was the highest when the temperature was up to 1200 K, which indicated that the heat resistance of poly(*para*-phenylene) obtained from benzene and biphenyl was poorer in relation to PPh. All of these results imply the higher thermal stability of PPh. The better heat resistance of PPh is of special significance for special applications where high thermal stability is essential.

### Conductivity and morphology

The conductivity of the PPh film obtained from BFEE was measured to be  $2.2 \times 10^{-3}$  S/cm; these values were higher than values obtained by the chemical method ( $10^{-9}$ – $10^{-6}$  S/cm).<sup>8</sup> According to the literature,<sup>8</sup> the conductivity of pristine chemically prepared PPh was less than  $10^{-9}$  S/cm as measured with pressed polymer pellets, and the conductivity of iodine-doped PPh (exposure of the polymer pellet to a vapor of iodine gives an iodine-doped sample) was in the range of  $10^{-6}$  S/cm. Moreover, the doping levels of as-prepared PPh films were determined under the conditions of different deposition charge densities (85–360 mC/cm<sup>2</sup>) to be close to 16%, which was lower than that of common conducting polymers, such as 25–35% for doped polypyrrole or polythiophenes. This factor contributed mainly to the low conductivity of the as-prepared PPh film compared to polypyrrole or polythiophenes ( $>10^2$  S/cm).

SEM of the PPh film is shown in Figure 9. The polymer film was compact and resembled ordered arrangements of the granules with a grain size of several hundred nanometers, and the growth of the nuclei was in the form of clusters [Fig. 9(A)]. Microscopically, the polymer film was made up of irregular micrometer and nanometer balls, which overlapped each other [Fig. 9(B,C)]. This morphology may facilitate the movement of doping anions into and out of the polymer film during the doping and dedoping process, in good agreement with the higher redox activity of the PPh films (Fig. 3). This also confirmed the high-quality PPh prepared in BFEE.

### CONCLUSIONS

High-quality PPh film with a conductivity of  $2.2 \times 10^{-3}$  S/cm was directly electrochemically synthesized in BFEE. The oxidation potential of Ph in this medium was determined to be only 1.35 V versus SCE. As-formed PPh films showed good redox activity and a high redox stability. FTIR spectra and <sup>1</sup>H-NMR spectra showed that the polymer chains were grown mainly via the coupling of the monomer at the C<sub>(2)</sub> and C<sub>(7)</sub> positions. The TGA results indicate that PPh films with a better thermal stability were obtained. The fluorescence spectra suggested that soluble PPh was a good blue-light emitter. All of these results indicate that PPh has some potential application in various fields, such as electron-transporting materials in LEDs and electroluminescent materials.

### References

1. Goldenberg, L. M.; Lacaze, P. C. *Synth Met* 1993, 58, 271.
2. Klaerner, G.; Lee, J. I.; Davey, M. H.; Miller, R. D. *Adv Mater* 1999, 11, 115.
3. Byun, H. Y.; Chung, I. J.; Shim, H. K.; Kim, C. Y. *Chem Phys Lett* 2004, 393, 197.
4. Madjarova, G.; Yamabe T. *J Phys Chem B* 2001, 105, 2534.
5. Nie, G.; Han, X.; Zhang, S.; Wei, Q. *J Polym Sci Part A: Polym Chem* 2007, 45, 3929.
6. Skotheim, T. A. *Handbook of Conducting Polymers*; Marcel Dekker: New York, 1986.
7. Aeiayach, S.; Lacaze, P. C. *J Polym Sci Part A: Polym Chem* 1989, 27, 515.
8. Saito, N.; Kanbara, T.; Sato, T.; Yamamoto, T. *Polym Bull* 1993, 30, 285.
9. Yamamoto, T.; Asao, T.; Fukumoto, H. *Polymer* 2004, 45, 8085.
10. Lu, B.; Zeng, L.; Xu, J.; Nie, G.; Cai, T. *Acta Chim Sinica* 2008, 66, 1593.
11. Shi, G.; Jin, S.; Xue, G.; Li, C. *Science* 1995, 267, 994.
12. Shi, G.; Li, C.; Liang, Y. *Adv Mater* 1999, 11, 1145.
13. Shi, G.; Xue, G.; Li, C.; Jin, S.; Yu, B. *Macromolecules* 1994, 27, 3678.
14. Nie, G.; Cai, T.; Xu, J.; Zhang, S. *Electrochem Commun* 2008, 10, 186.
15. Nie, G.; Cai, T.; Qu, L.; Xu, J.; Wei, Q.; Zhang, S. *J Electroanal Chem* 2008, 612, 191.
16. Zhang, S.; Nie, G.; Han, X.; Xu, J.; Li, M.; Cai, T. *Electrochim Acta* 2006, 51, 5738.
17. Chen, W.; Xue, G. *Prog Polym Sci* 2005, 30, 783.
18. Longchamp, S.; Caullet, C. *Electrochim Acta* 1984, 29, 1075.
19. Zimmermann, C.; Mohr, M.; Zipse, H.; Eichberger, R.; Schnabel, W. *J Photochem Photobiol A* 1999, 125, 47.
20. Tasi, F. C.; Chang, C. C.; Liu, C. L.; Chen, W. C.; Jenekhe, S. A. *Macromolecules* 2005, 38, 1958.
21. Zhou, M.; Heinze, J. *Electrochim Acta* 1999, 44, 1733.
22. Chen, X. W.; Inganäs, O. *J Phys Chem* 1996, 100, 15202.
23. Vorotyntsev, M. A.; Badiali, J. P. *Electrochim Acta* 1994, 39, 289.
24. Inzelt, G.; Pineri, M.; Schultze, J. W.; Vorotyntsev, M. A. *Electrochim Acta* 2000, 45, 2403.
25. Maarouf, E. B.; Billaud, D.; Hannecart, E. *Mater Res Bull* 1994, 29, 637.
26. Uckert, F.; Tak, Y. H.; Müllen, K.; Bässler, H. *Adv Mater* 2000, 12, 905.